Journal of Experimental and Theoretical Physics, Vol. 99, No. 6, 2004, pp. 1223–1232.
Translated from Zhurnal Éksperimental'noĭ i Teoreticheskoĭ Fiziki, Vol. 126, No. 6, 2004, pp. 1402–1412.

SOLIDS
Electronic Properties

Andreev States and Shot Noise in Bicrystal Junctions of Cuprate Superconductors

I. V. Borisenko, K. Y. Constantinian*, Yu. V. Kislinskiĭ, and G. A. Ovsyannikov

Institute of Radio Engineering and Electronics, Russian Academy of Sciences, Moscow, 125009 Russia

**e-mail: karen@hitech.cplire.ru*

Received February 6, 2004

Abstract—Experimentally observed features of the electrical and noise characteristics of bicrystal junctions of cuprate superconductors, such as linearity of the critical current density versus square root of the junction transparency and increase in the spectral density of shot noise for small bias voltages (below the superconducting gap), indicate that the superconducting current in cuprate bicrystal junctions is determined by the passage of quasi-particles through a potential barrier at the superconductor boundaries. This process involves bound states appearing as a result of multiple Andreev reflections in superconductors with dominant wavefunction components of the $d_{x^2-y^2}$ symmetry type. At the same time, interpretation of the experimental current–phase and current–magnetic field curves requires that the character of faceting at the bicrystal junctions would be also taken into account. © *2004 MAIK "Nauka/Interperiodica".*

1. INTRODUCTION

Shortly after the discovery of the Josephson effect, according to which Cooper pairs penetrate through a thin insulator layer (potential barrier) between two superconductors, it was pointed out [1] that the superconducting current I_S is proportional to the probability of electron tunneling, or the barrier transparency D, averaged over directions of the carrier momentum: $I_S \propto D$. Note that this behavior differs from that expected for a two-particle process, in which case the current would be proportional to D^2. Thus, the superconducting current I_S is on the same order of magnitude as the normal (single-particle) current ($I_N \propto D$). In this context, it was suggested [1] that the transport of Cooper pairs is a complex process proceeding via an "intermediate" electron–hole state in which the pair are dissociated so that the barrier transparency for such a pair is the same as that for single charge carriers. It was theoretically established, first for the superconductor–normal metal–superconductor (SNS) junctions [2] and somewhat later (in the 1990s) for the superconductor–insulator–superconductor (SIS) junctions [3], that these intermediate states are related to multiple Andreev reflections in superconductors.

In the case of tunneling junctions with a small transparency of the boundary, the midgap states (called the Andreev bound states) have energies close to the superconducting gap width Δ. In SNS junctions (with $D \approx 1$ [2]), as well as in the tunneling junctions involving cuprate superconductors with dominating wavefunction components of the $d_{x^2-y^2}$ symmetry type (D-type superconductors), Andreev levels occur near the Fermi surface (low-energy levels) [4–6]. Since the superconducting current is determined by the derivative of the level energy with respect to the phase difference φ of the wavefunctions of superconductors [7], the behavior of superconducting currents in DID and SNS junctions differ from that in SIS junctions. In particular, SNS junctions are characterized by the critical current $I_c(T)$ linearly increasing in a broad temperature range, whereas the temperature dependence of the critical current in SIS junctions rapidly reaches saturation [8]. In addition, the behavior of $I_c(T)$ in DID junctions depends on the orientation of D-type superconductors [5, 9, 10].

The influence of Andreev states on the phase and temperature dependences of the critical current in bicrystal junctions of cuprate superconductors has been experimentally studied in [11–14]. Alff *et al.* [12] also observed peculiarities in the current–voltage characteristics of such junctions that were caused by the presence of low-energy Andreev levels. Previously, we have pointed out certain features in the properties of bicrystal junctions, related to the low-energy Andreev levels in bicrystal junctions of cuprate superconductors. These peculiarities were manifested both in the electrical characteristics of junctions [13, 14], and in the appearance of excess shot noise at small voltages in such contacts [15–18]. However, despite a large number of publications on the physical properties of contacts involving metal oxide superconductors with high critical temperatures (see, e.g., review [19] and references therein), no systematic experimental investigations into the features of shot noise in such systems have been performed so far. The $1/f$ type noise in a bicrystal junction was studied by Kawasaki *et al.* [20], but

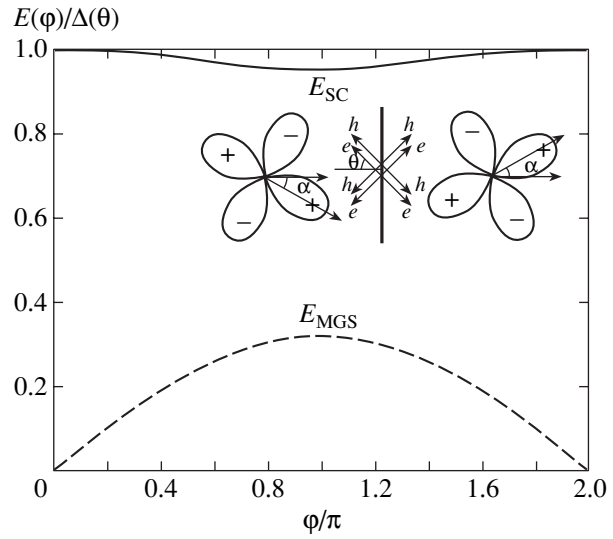

Fig. 1. The phase dependence of the energy of Andreev levels in a tunneling junction between S-type superconductors (solid curve) and the low-energy Andreev levels in a $D_\alpha ID_{-\alpha}$ junction (dashed curve) with a transparency of $D = 0.1$. The inset shows a schematic diagram of the bicrystal junction between two D-type superconductors with symmetric misorientation of the crystallographic axes relative to the direction of incidence of electrons and holes.

their data cannot be used to evaluate the effective transferred charge Q, which requires measurements of the shot noise to be performed at much higher frequencies. It should be noted that measurements of the spectral density of shot noise and the dependence of Q on the applied voltage provides additional information about the mechanism of charge transfer in the junction.

This paper presents the results of experimental investigations of the electrical and noise characteristics of bicrystal junctions of cuprate superconductors and considers the influence of low-energy Andreev bound states on the current transport in such junctions.

2. ANDREEV STATES IN SYMMETRIC SUPERCONDUCTING BICRYSTAL JUNCTIONS

It was theoretically established [2, 3] that, in the course of multiple Andreev reflections at the boundaries of usual (S-type) superconductors, one electron is reflected as a hole and the Cooper pair passes to a superconductor. The Andreev bound states are localized within a boundary layer at the interface, which has a thickness on the order of the coherence length. The energy of Andreev levels in the junctions between S-type superconductors can be expressed as

$$E_{SC} = \pm\Delta\sqrt{1 - D\sin^2(\varphi/2)}, \qquad (1)$$

where Δ is the superconducting energy gap width.

For junctions with a low transparency of the barrier ($D \ll 1$), the levels occur near the superconducting gap (Fig. 1). Most properties of the SIS junctions can be described both using the tunneling Hamiltonian model and in terms of the Andreev bound states.

The superconducting order parameter in a D-type superconductor changes sign when the momentum of a quasi-particle rotates by 90° (see the inset to Fig. 1). As a result, the phases of Andreev reflections in the junctions between D-type superconductors may have opposite signs for the incident and mirror-reflected quasi-particles. The sequence of mirror and Andreev reflections in the (110) plane leads to the formation of bound states with the energy E_{MGS} at the Fermi level [4]. On the current–voltage characteristics of junctions between a normal metal and a D-type superconductor (NID contacts), a peak in the density of states is manifested by anomalous conductivity observed at low applied voltage [21, 22].

The dependence of the energy of Andreev levels on the phase difference in a junction is determined by the angles of misorientation ($\alpha_{L(R)}$) of the crystallographic axes of D-type superconductors and by the angle of incidence (θ) of the quasi-particle. For mirror-symmetric ($\alpha_L = -\alpha_R = \alpha$) junctions ($D_\alpha ID_{-\alpha}$), the energy E_{MGS} of Andreev states for the angle $\alpha = 45°$ and the energy gap $\Delta_{R(L)} = \Delta_0\cos(2\theta + 2\alpha_{L(R)})$ (where $\Delta_0 = \Delta(\alpha = 0)$ depend on the phase as [5, 6]

$$E_{MGS} = \pm\Delta_{R(L)}\sin(\varphi/2)\sqrt{D(\theta)}. \qquad (2)$$

In contrast to the case described by Eq. (1), Andreev levels with the energies $E_{MGS}(\varphi)$ occur near the Fermi level even for $D \ll 1$, and their amplitudes do not exceed $\Delta_0\sqrt{D(\pi/4)}$.

Figure 2 shows the maximum energy of the Andreev bound states at $\varphi = \pi$ as a function of the incidence angle θ for various misorientation angles α in a symmetric junction with the typical transparency $D = 10^{-2}$. In the symmetric junction with $\alpha = 45°$, the low-energy Andreev states (E_{MGS}) are observed for all incident quasi-particles. As the misorientation angle decreases ($\alpha < 45°$), the angles θ for which the E_{MGS} levels are observed range within a 2α-wide interval relative to the directions $\theta = \pm\pi/4$. In other directions, the states with energies (E_{SC}) close to the energy gap appear. For $\alpha = 0$, the situation is close to that in the SIS junction, where the energies of Andreev states are described by formula (1).

Since the superconducting current is determined by the energies of Andreev states,

$$I_S \propto dE/d\varphi,$$

both contributions (1) and (2) should be taken into account for $0 < \alpha < 45°$ by adding the corresponding current components [6, 7, 11]. It should be noted that

the current is proportional to the first power of the transparency D for the states described by formula (1), and to the square root of D for the states described by formula (2). The cone (angular range) of tunneling, which determines the fraction of quasi-particles producing the main contribution to the current, can be either wide ($D(\theta) = D_0\cos\theta$, $D_0 = D(\theta = 0)$, for δ-shaped barriers), or rather narrow ($D \propto \exp(-2\theta)$ for thick barriers) [23]. In bicrystal junctions, the case of a thin barrier is more likely to take place, since the barrier thickness for superconducting current must not exceed the coherence length ξ_0.

3. METHODS OF PREPARATION AND CHARACTERIZATION OF SUPERCONDUCTING JUNCTIONS

3.1. Sample Preparation

The Josephson junctions were formed on $(1\bar{1}02)$-oriented Al_2O_3 bicrystal substrates with a misorientation angle of ±12° between the $\langle 11\bar{2}0\rangle$ crystallographic axes. The epitaxial films of $YBa_2Cu_3O_x$ (YBCO) cuprate with a thickness of 100–200 nm were grown at a substrate temperature of 750–770°C by means of cathode sputtering in an oxygen atmosphere at a pressure of 4 mbar. The cuprate films were deposited onto a CeO_2 buffer layer that was necessary to prevent the diffusion of aluminum from the substrate to the YBCO film at a high growth temperature. The 30-nm-thick epitaxial CeO_2 buffer layer was obtained by RF magnetron sputtering of a Ce target at 600–700°C in an $Ar–O_2$ gas mixture at a total pressure of 0.01 mbar. The epilayers were grown for the following epitaxial relations: $(001)YBCO/(001)CeO_2/(1\bar{1}02)Al_2O_3$ and $\langle 110\rangle YBCO/\langle 001\rangle CeO_2/\langle 11\bar{2}0\rangle Al_2O_3$. Then, 5-μm-long and 10-μm-wide bridges were formed in the YBCO film by means of ion-plasma etching and liquid-phase etching (0.5% Br_2 solution in ethanol) via a photoresist mask. In each sample, the bridges crossed the boundary at various angles γ (within 0–54°) relative to the normal to the interface. The deposition of CeO_2 film by sputtering a metallic Ce target, as well as the combined (ion-plasma and liquid-phase) etching of YBCO film, is an important original feature of the proposed technology [13, 14].

3.2. Methods of Measurements

The Josephson junctions obtained had the critical current density within $j_c = 10^4–10^5$ A/cm^2 and the characteristic voltage $V_0 = I_cR_N$ = 1–2 mV (R_N is the junction resistance in the normal state) at T = 4.2 K. The current–voltage characteristics of these junctions were measures in a range of temperatures (4.2 K < T < 77 K), magnetic fields ($H \le 100$ Oe), and under the action of a monochromatic microwave radiation with the frequency f_e = 30–100 GHz. In order to reduce the influence of external electromagnetic fields, all measurements were performed in a shielded room, with signal filtration in all leads connected to the samples. The critical temperatures of the superconducting films, as determined from the results of resistance measurements at an ac current below 1 μA, fell within T_c = 87–89 K.

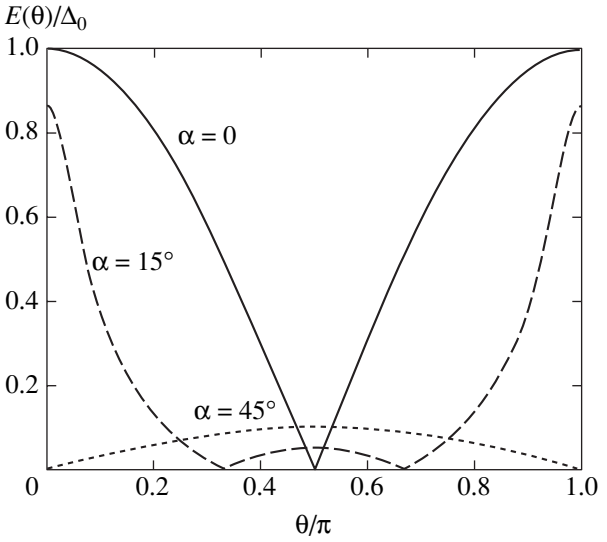

Fig. 2. Plots of the maximum energy of the Andreev bound states at $\varphi = \pi$ versus the quasi-particle incidence angle θ for various misorientation angles α in a symmetric bicrystal junction of D-type superconductors with a transparency of $D = 10^{-2}$.

The barrier layer transparency D (averaged over the momentum directions) was defined by the relation

$$D = \frac{2\pi^2\hbar^3}{e^2p_F^2}\frac{1}{R_NS} = \frac{2\rho l}{3R_NS}, \qquad (3)$$

where p_F is the Fermi momentum in YBCO, ρ is the resistivity of YBCO, l is the mean free path of electrons in the ab plane, and S is the contact area. For $\rho l = 4 \times 10^{-9}$ Ω cm^2 and the typical values of $R_NS = (1–3) \times 10^{-7}$ Ω cm^2, we obtain $D = (1–3) \times 10^{-2}$ [20, 22].

Figure 3 shows a schematic diagram of our experimental setup for the noise measurements. The measurements were performed in the decimeter wavelength range, where $1/f$ type noise is absent. The setup employed low-noise high-electron mobility transistors operating in the frequency range f_a = 1–2 GHz, with an intrinsic noise temperature of $T_{N1} = 8 \pm 2$ K and a gain of G_1 = 20 dB at T = 4.2 K. The balance input circuit ensured stable operation in a broad range of loads (10–100 Ω) and reduced the temperature of a background radiation reaching the sample via a coaxial cable. The noise temperature of the measuring circuitry contained contributions from the second amplification stage

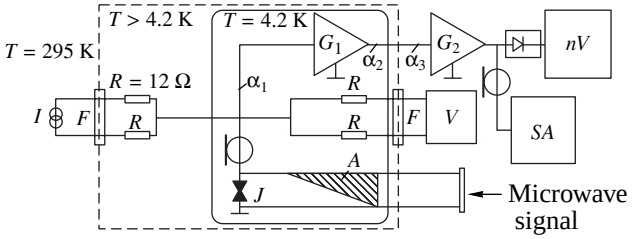

Fig. 3. Schematic diagram of the experimental setup for the noise measurements: (*J*) sample; (*I*) dc current source; (*V*) low-frequency voltage amplifier; (*F*) low-frequency filters; (*SA*) HP8563A spectrum analyzer; (G_1, G_2) first- and second-stage amplifiers; (*nV*) analog nanovoltmeter; diode symbol denotes a quadratic detector. Microwave signal is transmitted via a waveguide with cooled 20-dB attenuator *A* eliminating background irradiation of the sample.

(which occurred at room temperature and had an intrinsic noise temperature of T_{N2} = 130 K and a gain of G_2 = 40 dB) and the coaxial cable (with a damping coefficient of $\alpha_1 \le 0.2$ dB) connecting the sample to the low-noise amplifier. This amplifier was connected to the second-stage amplifier occurring at T = 300 K via a rigid coaxial cable in a stainless-steel braid. This cable could be considered as consisting of two parts: the first, with an effective temperature of $T_{T1} \approx 30$ K and a damping factor of $\alpha_2 \le 1.5$ dB, and the second, with $\alpha_3 \le 0.5$ dB at T_{T2} = 295 K (see Fig. 3). As a result, the total noise temperature of the measuring system was

$$T_0 \approx T_{N1} + \frac{1}{G}\left[T_{T1}(1-\alpha_2^{-1}) + T_{T2}(1-\alpha_3^{-1}) + \frac{T_{N2}}{\alpha_1+\alpha_2}\right] = 12 \text{ K},$$

which was on the same order of magnitude as the background radiation temperature ($T_b \approx 10$ K). Under conditions of good impedance matching between the sample junction and the low-noise amplifier, the accuracy of noise temperature determination was ±5 K. In order to minimize the influence of the background radiation reaching the sample via the rectangular waveguide, we used a cooled microwave absorber ensuring a 20-dB attenuation. The noise temperature of the measuring system was calibrated by varying the temperature of a 50-Ω-impedance matched load connected instead of the sample.

Parameters of bicrystal junctions measured at liquid helium temperature (T = 4.2 K)

Parameter	Sample			
	BC-9	BC-15	BC-16	BC-21
Misorientation angle α	33°	12°	12°	12°
I_c, μA	70	18	55	32
R_N, Ω	16	90	40	60
$R_N S$, Ω μm^2	10	45	20	30
Q_{max}/e	10	–	16	15
V_Q, μV	300 (H = 0)	–	30 (H = 65 Oe)	10 (H = 45 Oe)
ΔV, mV (for $Q \sim e$)	V > 4	25–70	20–60	5–20

The response signal voltage (proportional to the noise power P_N) was measured at the output of a quadratic detector. Simultaneously, the amplitude–frequency characteristic was measured at the amplifier output. The absence of resonance features on this characteristic in the course of noise measurements was evidence of a good impedance matching between the sample junction and the measuring circuit. By varying the inductance of the cable connecting the sample to the amplifier, it was possible to ensure nonresonance impedance matching in a broad range of normal resistances of the sample junctions (R_N = 15–90 Ω). However, exact quantitative determination of the spectral density of current fluctuations $S_I(V) \propto P_N/R_d$ (R_d is the differential resistance of the junction) and the corresponding effective transferred charge $Q(V) = S_I(V)/2I$ was possible only for the junctions with normal resistances within a narrower interval, R_N = 20–60 Ω. Data on the maximum effective transferred charge Q_{max}, the range of voltages ΔV where this charge was constant and equal to the electron charge, and the electric parameters of several junctions are presented in the table.

4. RESULTS AND DISCUSSION

4.1. Electrical Properties of Superconducting Bicrystal Junctions

Figure 4 shows the typical current–voltage characteristic of a bicrystal junction, which is well described by a resistive model with two channels of charge transfer, including the current of quasi-particles (V/R_N) and the superconducting current ($I_S(\varphi) = I_c \sin\varphi$). A small level of the excess current (deviation from the Ohm law) at voltages above 10 mV is evidence of the absence of direct (nontunneling) conductivity. However, the temperature dependence of the critical current (left inset to Fig. 4) is close to linear (to within the experimental accuracy), in contrast to a theoretical curve obtained for the tunneling junctions between S-type superconductors [8] that exhibits saturation for $kT < \Delta$. The junctions with direct conductivity, in which the low-energy Andreev states determine the superconducting current transport, usually exhibit an almost linear behavior of $I_c(T)$ in a broad temperature interval.

According to Fig. 2, the states of both types described by Eqs. (1) and (2) can be observed in the tunneling DID junctions depending on the incidence

angle of quasi-particles, and the superconducting current consists of two parts [6, 11]:

$$I_S(f) = I_{SC}(\varphi) + I_{MGS}(\varphi).$$

The contribution due to Andreev states near the gap, which is described by Eq. (1), rapidly increases with the temperature (in proportion to $\Delta^2(T)$ according to the Ambegaokar–Baratoff law [8]) and exhibits saturation at low temperatures:

$$I_{SC} \propto D_0\Delta_0\cos(2\alpha)\sin\varphi.$$

The contribution due to states near the Fermi level increases in proportion to $1/T$ with decreasing temperature and (for $kT \ll \Delta\sqrt{D}$) saturates at

$$I_{MGS} \propto -\Delta_0\sin(2\alpha)D_0\cos\frac{\varphi}{2}\mathrm{sgn}\left(\sin\frac{\varphi}{2}\right)$$

(with the minus sign). Therefore, there must exist a certain temperature T^* at which the $I_c(T)$ curve exhibits a dip and the $I_S(\varphi)$ curve deviates from the sinusoidal law. For a barrier with the transparency $D = 10^{-2}$ and an YBCO superconducting gap of $\Delta_0 = 20$ meV, the estimation yields $T^* = 12$ K. The typical experimental curve of $I_c(T)$ presented in the left inset to Fig. 4 exhibits no such dip, which is probably related to faceting developed at the interface during epitaxial growth [19, 22]. Il'ichev *et al.* [11] studied bicrystal junctions of small thickness (comparable with the facet size) and observed a dip in $I_c(T)$ for a temperature at which the current versus phase curve deviates from the sinusoidal law. A nonmonotonic $I_c(T)$ curve was also observed for junctions of rather large thickness (on the order of several microns), but only for asymmetric bicrystal junctions [24].

At high temperatures ($T_c - T \ll T_c$), where the influence of thermal fluctuations is large, the temperature dependence of I_c is close to $(T_c - T)^{1/2}$ [6, 25]. This temperature interval features the most pronounced suppression of the D-type component of the order parameter near the bicrystal junction [26].

According to Eqs. (1) and (2), the superconducting current at $T \ll T_c$ depends on the transparency D in the DID junctions ($I_c \propto \sqrt{D}$) not in the same manner as in the SIS junctions ($I_c \propto D$). This difference is related to the fact that low-energy Andreev levels in the DID junctions occur at the Fermi level ($E \sim \Delta\sqrt{D}$, see formula (2)), whereas these levels in S-type superconductors occur near the gap ($E \sim \Delta$, see formula (1)). The behavior observed in our experiments seems more like it obeys the root law: $I_c \propto 1/\sqrt{R_N S} \propto \sqrt{D}$ (see the right inset to Fig. 4). Despite a rather large scatter of experimental points (characteristic of the junctions involving cuprate superconductors [19]), the best fit (minimum deviation) of $I_c(D)$ was observed for the $I_c \propto \sqrt{D}$ curve. We believe that the observed dependence of the energy of Andreev levels on the junction transparency is quite stable to the action of various factors, including the boundary faceting, which leads to the appearance of both symmetric ($D_\alpha ID_{-\alpha}$) and asymmetric ($D_\alpha ID_0$ junctions). However, the $D_\alpha ID_{-\alpha}$ junctions according to formula (2) at low temperatures have $I_S \propto \Delta_0 D_0$, whereas the $D_\alpha ID_0$ junctions are characterized by $I_S \propto \Delta_0 D_0^2$ [5]. Therefore, the superconducting current for $D_0 < 1$ is determined by the regions with symmetric misorientation of the crystallographic axes.[1] It is not excluded that, in the case of suppression of the order parameter, the D-type component may influence the behavior of $I_c(D)$ [26]. It should be noted that a dependence of the $I_c \propto \sqrt{D}$ type was theoretically predicted for SIS contacts with a thick potential barrier [28]. For such SIS junctions, the difference of the spectrum of the Andreev bound states from the spectrum according to Eq. (1) leads to a different dependence of I_c on the barrier transparency. However, realization of the mechanism described in [28] requires low transparency of the boundary ($D \le 10^{-8}$) and weak influence of the depairing factors on the density of states.

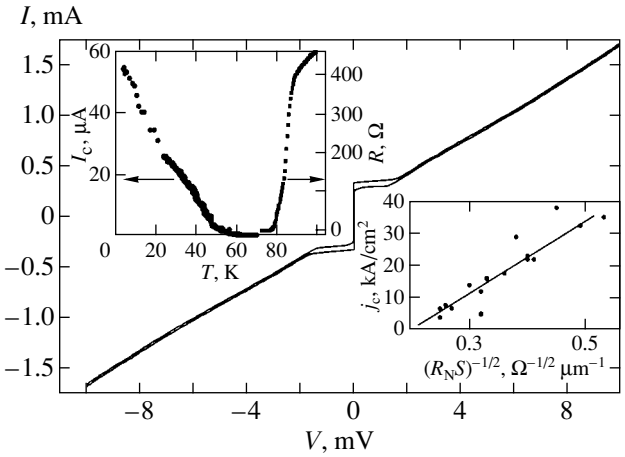

Fig. 4. The typical current–voltage characteristic of a bicrystal junction measured at $T = 4.2$ K. The left inset shows the temperature dependence of the critical current I_c and the resistance R; the right inset shows a plot of the critical current density versus characteristic normal resistance (R_NS) of the junction.

[1] Inhomogeneity (roughness) of the bicrystal junction on a smaller scale (on the order of the Fermi wavelength of quasi-particles ($\lambda_F \approx 0.01$ μm) breaks the coherence of Andreev reflections for small incidence angles of quasi-particles ($4\pi\eta(\lambda)\cos\theta > \pi$, where η is the characteristic size of the junction inhomogeneity in the direction of current flow [27].)

4.2. The Dependence of the Critical Current on the Magnetic Field

Figure 5 presents the experimental dependence of the critical current on the magnetic field, $I_c(H)$, for one of the bicrystal junctions studied. As can be seen, the curve is significantly different from the Fraunhofer diffraction pattern typical of junctions with a small characteristic inhomogeneity size, $w < \lambda_J$ (in this case, w is the width of bridges crossing the bicrystal junction), where λ_J is the Josephson penetration depth [8]. The observed $I_c(H)$ curve can be related to inhomogeneity (roughness) of the junction related to faceting at the interface: previously, such patterns were observed for the misorientation angles greater than 10° (but smaller than 45°) [29]. It was demonstrated [30] that the experimental behavior presented in Fig. 5 could be well described in terms of a system of parallel Josephson junctions with a certain distribution of critical currents. Some bicrystal junctions exhibited $I_c(H)$ curves in which the ratio of the critical current to local maximum was below two and the subsequent $I_c(H)$ peaks weakly decreased with increasing magnetic field. It was shown [30] that the junctions of this kind have to be considered with regard to the presence of facets possessing the properties of π-contacts [6, 25].

4.3. The Phase Dependence of the Critical Current

The phase dependence of the superconducting current, $I_S(\varphi)$, in a Josephson junction is determined by the character of conductivity between two superconductors in contact with each other. At relatively high temperatures ($T_c - T \ll T_c$), the $I_S(\varphi)$ curve shape is very close to sinusoidal for the junctions of any type: $I_S(\varphi) = I_c \sin\varphi$. This dependence is retained in all low-transparency SIS junctions ($D \ll 1$) at low temperatures ($T \ll T_c$) [1, 5, 8], while in thick SNS junctions ($L > h v_F/kT$) this law holds for $T < T_c$. In order to reveal deviations of the $I_S(\varphi)$ curve shape from sinusoidal, we have measured the current–voltage characteristics of bicrystal junctions exposed to a monochromatic microwave radiation $A\sin(2\pi f_e t)$ in the millimeter range (f_e = 40–100 GHz) [14]. The experiments were performed for the junctions featuring both symmetric (the bridge was perpendicular to the interface) and asymmetric current flow (the bridge was oriented at γ = 0–72° relative to the interface). Previously, the appearance of the subharmonic Shapiro steps in the junctions with nonsinusoidal $I_S(\varphi)$ curve was used to study the phase dependence of the critical current of thin tin bridges [31] and hybrid Pb/Au/YBCO superconducting heterojunctions [32].

Figure 6 presents the dependences of the first ($I_1(A)$) and subharmonic ($I_{1/2}(A)$) Shapiro steps on the radiation amplitude for the bicrystal junctions with $\gamma = 0$ and 54°. The inset to Fig. 6 shows theoretical curves calculated using a resistive model for $f_e > 2eI_cR_N/h$. The calculations were performed for the sinusoidal relation

$$I_S(\varphi) = I_c \sin\varphi$$

and for a system with small deviation from the sinu-

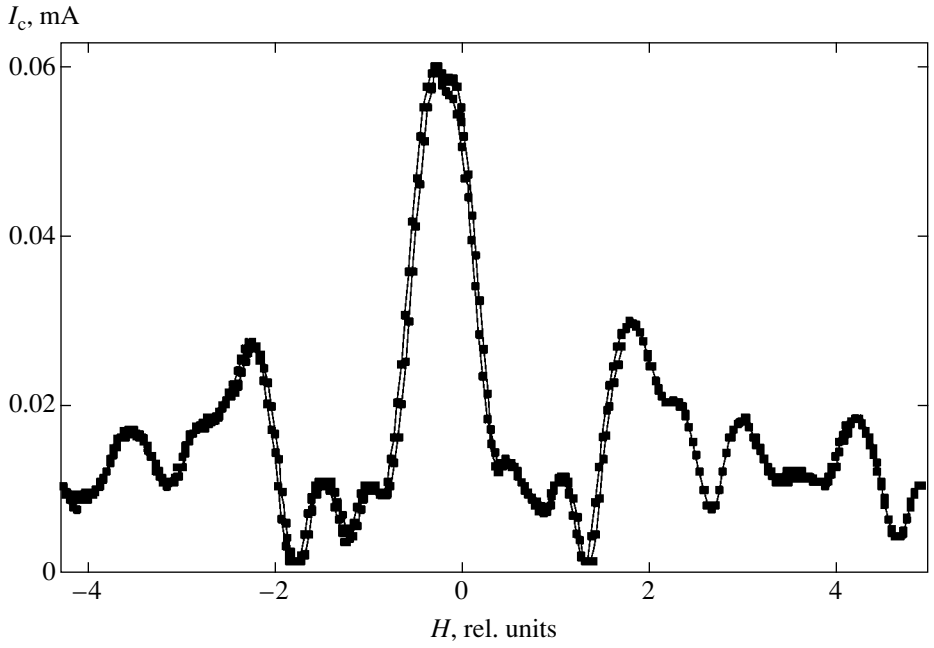

Fig. 5. Experimental curve of the critical current versus magnetic field applied to a bicrystal junction.

soidal law:

$$I_S(\varphi) = (1-\delta)I_c\sin\varphi + \delta I_c\sin(2\varphi), \quad \delta = 0.2.$$

As can be seen, the difference between the two theoretical and experimental $I_1(A)$ curves is relatively small. However, even a small deviation of the phase dependence from sinusoidal leads to the appearance of noticeable subharmonic Shapiro steps. The results of experimental measurements of the amplitude of subharmonic steps as a function of the bridge orientation angle γ showed the absence of $\sin(2\varphi)$ components in the angular interval $\gamma = 0$–$36°$ (to within 5%). For the angles $\gamma > 40°$, the contribution of $\sin(2\varphi)$ exhibits monotonic growth.[2]

The deviation of the phase dependence from sinusoidal for the bicrystal junctions with asymmetric bias current is probably related to the current component along the bicrystal interface, which changes the spectrum of low-energy Andreev states. The maximum energy of Andreev states, $\Delta_0\sqrt{D_0} \approx 2$ meV, is comparable to the value ($\varepsilon = e v_F j_S \lambda^2 \approx 5$ meV) of the longitudinal component of the superconducting current for $j_S = 10^3$ A/cm^2, $v_F = 5\times10^4$ cm/s, and $\lambda = 0.1$ μm (here, λ is the London penetration depth).

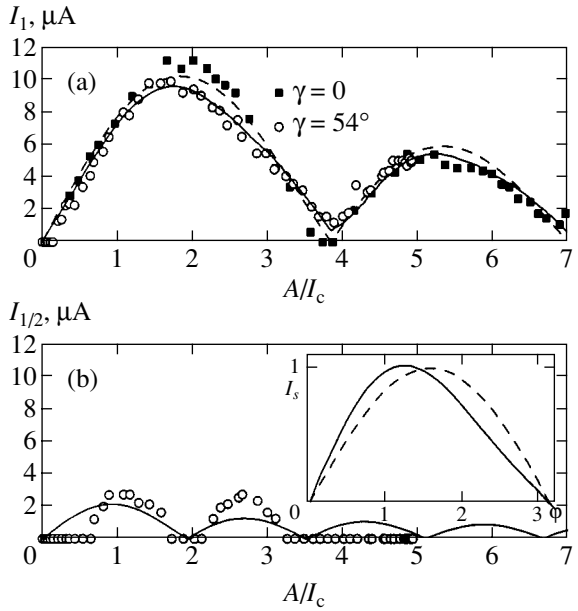

Fig. 6. Plots of (a) the first and (b) the subharmonic Shapiro steps versus microwave radiation amplitude (f_e = 100 GHz, T = 4.2 K). Curves show the dependences calculated using the resistive model for $I_S(\varphi) = I_c\sin\varphi$ (dashed) and $I_S(\varphi) = (1-\delta)I_c\sin\varphi + \delta I_c\sin 2\varphi$ ($\delta = 0.2$) (solid); symbols present the experimental data for two orientations of bridges. The inset shows the corresponding $I_S(\varphi)$ curves.

4.4. Shot Noise in Bicrystal Junctions

Indirect evidence for the existence of excess nonthermal noise in the junctions involving cuprate superconductors has been obtained from data on the broadening of the line of intrinsic Josephson generation [33, 34] and on the noise characteristics of SQUIDs and electromagnetic radiation detectors [35]. However, the $1/f$ type fluctuations do not always explain the growth of noise (in particular, for processes in the microwave frequency range). From this standpoint, it was of interest to study the appearance of shot noise—a factor determining both broadening of the generation line and deterioration of the device characteristics.

The noise characteristics of junctions were studied both in the autonomous regime ($H = 0$, $A = 0$) and in a weak magnetic field ($H < 100$ Oe) sufficient to suppress the critical current in the junction. Figure 7 shows the current–voltage characteristic and the noise power as a function of the bias voltage, $P_N(V)$), in the autonomous regime.[3] In the region of large voltages ($V > 30$ mV),

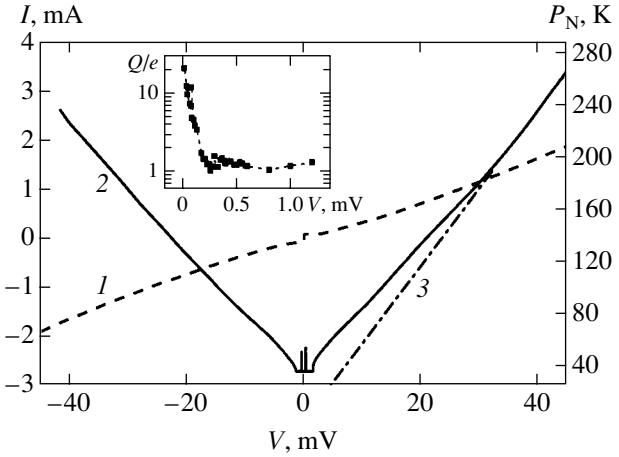

Fig. 7. Symmetric bicrystal junction: (*1*) current–voltage characteristic at T = 4.2 K; (*2*) noise power $P_N(V)$ expressed in kelvins; (*3*) theoretical shot noise temperature $T_{SH}(V) = (e/2k)I(V)R_d$. The inset shows the normalized effective charge $Q(V) = S_I(V)/2I$.

the experimental $P_N(V)$ curve coincides with the classical dependence of the shot noise temperature,

$$T_{SH}(V) = (e/2k)I(V)R_d,$$

where R_d is the differential resistance of the junction.

[2] For a high-frequency external action ($f_e > 2eI_cR_N/h$), the ratio of the maximum amplitude of the subharmonic step to the critical current within the framework of the resistive model is equal to the ratio of the second and first harmonics in the phase dependence of the critical current.

[3] The noise power is expressed in the temperature units due to the special features of calibration of the experimental setup described in Section 3.2.)

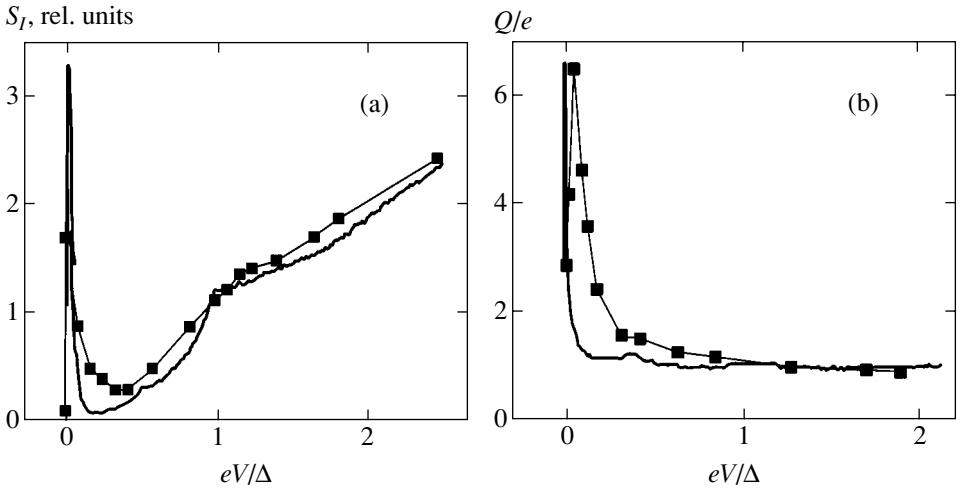

Fig. 8. (a) Spectral density of the noise current $S_I(V)$ at $T = 4.2$ K for a bicrystal junction with $R_N = 18\ \Omega$ (squares represent experimental data; the thick solid curve shows the results of theoretical calculation for a DID junction with $D = 0.01$ and $e\Delta_0 = 5$ mV [18]); (b) normalized effective charge $Q(V) = S_I(V)/2I$ (squares present experimental data; thick solid curve shows the results of theoretical calculation).

Calculations of $Q(V)$ were performed for the spectral density of noise $S_I = 2eI$ at $eV > kT, hf$ (this condition was satisfied in the experiment for $V > 0.7$ mV at $T = 4.2$ K and the amplifier operating at $f_a = 1$–2 GHz). Previously, an analogous dependence (similar to the curve in Fig. 7) of the spectral density of noise in a superconducting junction was observed for SIS contacts [36–39] in the region of voltages above Δ/e.

As can be seen from Fig. 7, the junction noise temperature T_N exceeds the shot noise temperature $T_{SH}(V)$ in a broad range of lower voltages ($0 < V < 30$ mV). In the region of small voltages ($V < 2$ mV) the $T_N(V)$ curve exhibits peaks caused by the appearance of the intrinsic Josephson radiation at the amplifier input. At small voltages, a sharp increase in the value of $R_d(V)$ (this dependence is not depicted in Fig. 7) affects impedance matching between the sample and amplifier. For this reason, below we will consider only the spectral density of shot noise $S_I(V) \propto 4kT_N/R_d$ and the effective charge $Q(V) = S_I(V)/2I$, since these quantities are independent of R_d. Taking into account variation of the $R_d(V)$ value, we observe an almost linear increase in $S_I(V)$ at $V > 4$ mV and a distinct peak at $V < 2$ mV. The inset to Fig. 7 shows the effective charge variation in the same junction, which reveals the growth in $Q(V)$ that is characteristic of the superconductor structures featuring multiple Andreev reflections [15–18]. The ratio Q_{max}/e exceeded ten (see table).

Figure 8 shows $S_I(V)$ and $Q(V)$ curves measured in the presence of an external constant magnetic field decreasing I_c and R_d of the junction. At a large bias voltage ($V > 10$ mV), the $S_I(V)$ curves observed in the magnetic field (Fig. 8a) and at $H = 0$ (Fig. 7) coincide, which allows us to use the noise density calibration performed for $S_I(V)$ in the autonomous regime.[4] As can be seen, the R_d variations at small bias voltages do not influence the shape of the curve of transferred charge versus voltage (Fig. 8b). The bias voltage in Fig. 8 is normalized to $V = \Delta_0/e = 5$ mV and the experimental values of S_I and Q are expressed in relative units. Solid curves show the results of theoretical calculations for a mirror-symmetric junction $D_{45}ID_{-45}$ with $D = 0.1$ at a fixed value of the inelastic scattering parameter (0.003Δ). As can be seen, the experimental data fit to the theory well taking into account multiple Andreev reflections in the junctions involving D-type superconductors [18]. However, the values of the transparency and gap evaluated for the D-type superconductor using this comparison to the theory differ from the values determined using electrical measurements. It should be also noted that we did not observe subharmonic gap features on the current–voltage characteristic predicted in [18], which is probably related to the low transparency of the junction.

At the same time, the values of V_Q for which $Q(V) = Q_{max}$ in the magnetic field proved to be much lower than in the autonomous regime. The measurements for the autonomous transitions could be performed only for the junctions with low values of the normal resistance ($R_N < 20\ \Omega$), which were poorly impedance-matched to the measuring amplifier. As a result, the error in these measurements exhibited a severalfold increase. For such

[4] The range of voltages for which the shot noise obeys the classical relation $Q = e$ changed from one sample to another. The upper boundary of this range is probably related to the potential barrier height (see table).

junctions, comparison of theory and experiment [18] was performed using normalized dependences.

The fact that the intensity of noise caused by multiple Andreev reflections exceeds the level of thermal fluctuations explains the experimentally observed broadening of the Josephson generation line in the junctions of cuprate superconductors [33–35]. This result should be taken into account in applications based on the Josephson effect. Note also that, in the region of high bias voltages, the Nyquist noise in the junction is much lower than the shot noise.

5. CONCLUSIONS

The results of our experimental study of the critical current as a function of the temperature, transparency, and phase difference between superconducting electrodes, as well as the measured current–voltage characteristics showed that the most probable mechanism of superconducting current transport in bicrystal junctions of cuprate superconductors is electron tunneling through the barrier with participation of the bound states formed at the superconductor-insulator interface as a result of multiple Andreev reflections. However, the shapes of the experimental current–phase and current–magnetic field curves cannot be described within the framework of a homogeneous junction model, without taking into account the roughness caused by faceting at the interface in the course of epitaxial layer growth. At present, there is no consistent theory adequately describing the experimental situation. In the region of relatively large bias voltages ($V > 5$ mV), the junction noise level exceeds the level of thermal fluctuations, in agreement with the voltage dependence of the shot noise in the junction (analogous to that observed for the junctions of S-type superconductors). In the region of small voltages, a noise peak is observed that is characteristic of superconducting junctions featuring multiple Andreev reflections.

ACKNOWLEDGMENTS

The authors are grateful to F.V. Komissinski, V.K. Kornev, and P.B. Mozhaev for their help in conducting experiments and to Yu.S. Barash, A.V. Zaitsev, A. Kadigrobov, J. Mygind, N. Pedersen, and V. Shumeĭko for fruitful discussions of results.

This study was supported in part by the Federal Program “Current Problems in Physics of Condensed State” (“Superconductivity” Subprogram), the Presidential Program of Support for Leading Scientific Schools in Russia (project no. NSh-1344.2004.2), the Russian Foundation for Basic Research (project no. 04-02-16818a), the INTAS Foundation (grant no. 2001-0809), and the International Scientific-Technological Center (grant no. 2369).

REFERENCES

1. I. O. Kulik and I. K. Yanson, in *Josephson Effect in Superconducting Tunnel Structures* (Nauka, Moscow, 1970) [in Russian].
2. I. O. Kulik, Zh. Éksp. Teor. Fiz. **57**, 1745 (1969) [Sov. Phys. JETP **30**, 944 (1970)].
3. A. Furusaki and M. Tsukada, Phys. Rev. B **43**, 10164 (1991).
4. C.-R. Hu, Phys. Rev. Lett. **72**, 1526 (1994).
5. R. A. Riedel and P. F. Bagwell, Phys. Rev. B **57**, 6084 (1998).
6. Yu. S. Barash, Phys. Rev. B **61**, 678 (2000).
7. C. W. Benaker, Phys. Rev. Lett. **67**, 3836 (1991).
8. K. K. Likharev, Rev. Mod. Phys. **51**, 101 (1979).
9. Y. Tanaka and S. Kashiwaya, Phys. Rev. B **53**, 11957 (1996).
10. Yu. S. Barash, H. Burkhardt, and D. Rainer, Phys. Rev. Lett. **77**, 4070 (1996).
11. E. Il’ichev, M. Grajcar, R. Hlubina, *et al.*, Phys. Rev. Lett. **86**, 5369 (2001).
12. L. Alff, A. Beck, R. Gross, *et al.*, Phys. Rev. B **58**, 11197 (1998).
13. G. A. Ovsyannikov, A. D. Mashtakov, I. V. Borisenko, and K. Y. Constantinian, J. Low Temp. Phys. **117**, 605 (1999).
14. A. D. Mashtakov, K. Y. Constantinian, G. A. Ovsyannikov, and E. A. Stepantsov, Pis’ma Zh. Tekh. Fiz. **25** (7), 1 (1999) [Tech. Phys. Lett. **25**, 249 (1999)].
15. E. V. Bezuglyi, E. N. Bratus’, V. S. Shumeiko, and G. Wendin, Phys. Rev. Lett. **83**, 2050 (1999).
16. Y. Naveh and D. V. Averin, Phys. Rev. Lett. **82**, 4090 (1999).
17. K. Y. Constantinian, G. A. Ovsyannikov, I. V. Borisenko, *et al.*, IEEE Trans. Appl. Supercond. **13**, 610 (2003).
18. J. C. Cuevas and M. Fogelström, Phys. Rev. B **64**, 104502 (2001); Phys. Rev. Lett. **89**, 227003 (2002).
19. H. Hilgenkamp and J. Mannhart, Rev. Mod. Phys. **74**, 485 (2002).
20. M. Kawasaki, P. Chaudhari, and A. Gupta, Phys. Rev. Lett. **68**, 1065 (1992).
21. M. Covington, M. Aprili, E. Paraoanu, *et al.*, Phys. Rev. Lett. **79**, 277 (1997).
22. F. V. Komissinski, G. A. Ovsyannikov, Yu. V. Kislinskiĭ, *et al.*, Zh. Éksp. Teor. Fiz. **122**, 1247 (2002) [JETP **95**, 1074 (2002)].
23. T. Lofwander, V. S. Shumeiko, and G. Wendin, Supercond. Sci. Technol. **14**, R53 (2001).
24. Z. G. Ivanov, E. A. Stepantsov, A. Y. Tzalenchuk, *et al.*, IEEE Trans. Appl. Supercond. **3**, 2925 (1993).
25. H. Hilgenkamp, J. Mannhart, and B. Mayer, Phys. Rev. B **53**, 14586 (1996).
26. L. J. Buchholtz, M. Palumbo, D. Rainer, and J. A. Sauls, J. Low Temp. Phys. **101**, 10789 (1995).
27. M. B. Walker and P. Pairor, Physica C (Amsterdam) **341**–**348**, 1523 (2000).

28. G. Wendin and V. S. Shumeiko, Phys. Rev. B **53**, R6006 (1996).
29. F. V. Komissinski, G. A. Ovsyannikov, and Z. G. Ivanov, Fiz. Tverd. Tela (St. Petersburg) **43**, 769 (2001) [Phys. Solid State **43**, 801 (2001)].
30. V. K. Kornev, I. I. Soloviev, N. V. Klenov, *et al.*, IEEE Trans. Appl. Supercond. **13**, 825 (2003).
31. V. N. Gubankov, V. P. Koshelets, and G. A. Ovsyannikov, Zh. Éksp. Teor. Fiz. **71**, 348 (1976) [Sov. Phys. JETP **44**, 181 (1976)].
32. R. Kleiner, A. S. Katz, A. G. Sun, *et al.*, Phys. Rev. Lett. **76**, 2161 (1996).
33. L. É. Amatuni, R. M. Martirosyan, and K. Y. Constantinian, Pis'ma Zh. Tekh. Fiz. **20** (3), 86 (1994) [Tech. Phys. Lett. **20**, 128 (1994)].
34. Y. Y. Divin, U. Poppe, K. Urban, *et al.*, IEEE Trans. Appl. Supercond. **9**, 3346 (1999).
35. O. Harnack, M. Darula, S. Beuven, and H. Kohlstedt, Appl. Phys. Lett. **76**, 1764 (2000).
36. P. L. Richards and T.-M. Shen, Appl. Phys. Lett. **36**, 480 (1980).
37. Y. Blanter and M. Buttiker, Phys. Rep. **336**, 1 (2000).
38. P. Dieltman, H. G. Bukkems, T. M. Klapwijk, *et al.*, Phys. Rev. Lett. **79**, 3486 (1997).
39. K. Y. Constantinian, G. A. Ovsyannikov, I. V. Borisenko, *et al.*, Supercond. Sci. Technol. **14**, 1035 (2001).

Translated by P. Pozdeev